2014

Effect of Refrigerant Charge, Compressor Speed and Air Flow Through the Evaporator on the Performance of an Automotive Air Conditioning System

Santanu Prasad Datta
Indian Institute of Technology Kharagpur, India, santanu@mech.iitkgp.ernet.in

Prasanta Kumar Das
Indian Institute of Technology Kharagpur, India, pkd@mech.iitkgp.ernet.in

Siddhartha Mukhopadhyay
Indian Institute of Technology Kharagpur, India, smukh@ee.iitkgp.ernet.in

Effect of Refrigerant Charge, Compressor Speed and Air Flow through the Evaporator on the Performance of an Automotive Air Conditioning System

Santanu P. DATTA[*1], Prasanta K. DAS[1], Siddhartha MUKHOPADHYAY[2]

[1] Department of Mechanical Engineering,
Indian Institute of Technology Kharagpur, 721302, India
santanu@mech.iitkgp.ernet.in
pkd@mech.iitkgp.ernet.in

[2] Department of Electrical Engineering,
Indian Institute of Technology Kharagpur, 721302, India
smukh@ee.iitkgp.ernet.in

* Corresponding Author

ABSTRACT

Using identical mechanical hardware used in an automobile, a stationary test bench has been developed for an automotive air conditioning system (AACS). However, a number of additional sensors have been used in the system for an accurate assessment of its performance. The steady state performance of the system has been investigated for three independent variables, namely the refrigerant charge level, the compressor speed and the speed of the evaporator fan. Tests have been planned to estimate the performance of the individual components and to determine a non-dimensional rating parameter to describe condenser performance. While the refrigerant flow rate is influenced primarily by refrigerant charge level and compressor speed, the COP and cooling capacity depends on all the three operating variables. The optimum operating condition with compressor and blower speed along with refrigerant charge level has also been identified.

1. INTRODUCTION

During the last few decades research on Automotive Air Conditioning System (AACS) reached a milestone in terms of comfort, safety and economy. However investigation on system performance due to AACS's variable operating conditions is limited. The performance of any AACS mostly depends on compressor speed, blower speed, refrigerant charge level and ambient condition. However, the combined effect of these parameters on the performance of AACS could be non-intuitive. In the past decades considerable effort has been made for improving the performance of AACS by improving the hardware and by better control strategies (Bhatti, 1999; Kargilis, 2003). Kaynakli and Horuz (2003) have experimentally investigated the performance of a stationary AACS for a range of compressor speed, temperature of the evaporator and the condenser as well as the ambient temperature. The influence of compressor speed on the refrigerant mass flow rate was much prominent compared to the effect of evaporator and condenser temperature on it. An increase in air inlet temperature increases both the cooling capacity and COP of the system. Performance studies on AACS under stationary condition have also been made by Park et al. (1999), Gu et al. (2003), Wang and Gu (2004) and Wang et al. (2005).

Ratts and Brown (2000) investigated the thermodynamic losses in different components of a cycling clutch, orifice tube type AACS through a combination of experiment and second law analysis for different car speeds. Hosoz and Direk (2006) have developed a stationary R134a based AACS which can operate both on heat pump (air to air) and air conditioning modes. It was observed that the heat pump operation usually yielded a higher COP and a lower rate of exergy destruction. Qi et. al. (2007) have investigated a new displacement control for a variable displacement compressor in connection with an automotive air conditioning system.

Only limited efforts have been made for the theoretical analysis of automotive HVAC systems. Lee and Yoo (2000) developed a simulation program for an automotive air conditioning system to investigate the effect of condenser volume and the refrigerant charge quantity. It is reported that 10% overcharging resulted in the best performance of the system. In a similar kind of investigation, Jabardo et al. (2002) observed no effect of refrigerant

charge on system performance as the contradiction to that of Lee and Yoo (2000). Hosoz and Ertunc (2006), Atik et al. (2010) and Kamar et al. (2013) used artificial neural network (ANN) to predict the performance of a stationary AACS. Trzebinski and Szczygiel (2010) conducted a thermodynamic analysis of car air conditioning considering different cases like controlled and uncontrolled expansion valve as well as uncontrolled and externally controlled compressor. Effect of refrigerant charge and ambient temperature has also been studied.

In recent years, there have been increased concerns regarding energy efficient operation of AACS. Mainly the energy consumption by the compressor and the blower of the evaporator has been targeted and different control strategies have been postulated. So that a reduction in the energy demand can be achieved by maintain the comfort condition over a wide operating range. In a comprehensive study, Forrest and Bhatti (2002) proposed two methodologies namely the use of recirculated air and the reduction of reheat with a detail strategy of blower speed control. With a detail analysis and experimental study they established the feasibility of these two techniques. Khayyam along with his co-workers made some consolidated study for the energy optimization of AACS using different control strategies including neural network (Khayyam et al., 2011) and fuzzy logic (Khayyam et al., 2012). In these works he attempted the control of recirculated and fresh air as well as a close co-ordination between the engine and the air conditioning system to achieve the energy economy. In a recent paper (Khayyam, 2013) it is proposed to include a feedback even from the road condition to reduce the energy demand of the air conditioner.
The above review brings out the following points:

- Time to time some initiatives has been taken to study the performance of car air conditioning systems mostly under steady state conditions.
- Experimental set ups are invariably stationary facilities which resemble specific automotive systems up to different degrees.
- The performance of an AACS depends on many parameters namely, compressor speed, refrigerant charge, blower speed, ambient condition etc. However, most of the works consider the variation of only a limited number of parameters.
- Based on the experimental results and theoretical analyses, it is found that multiple factors can cause inaccuracies in charge prediction like, unaccounted liquid volumes, refrigerant dissolved in the compressor lubricant, inaccurate void fraction models, and an inaccurate estimate of the subcooled liquid length.
- The reported experimental results are system specific with variation of parametric range and type of components.

The objective of the present work is to study the effect of three main process parameters namely, compressor speed, refrigerant charge, and blower speed on the performance of an AACS through an elaborate set of experiments. It is intended to investigate the effects of these parameters on the temperature and pressure at the suction and discharge side. Further, the variation of cooling capacity, compression work and system COP has also been examined. An effort has been made to evaluate the performance of the condenser from the thermograph of its surface. Finally, the point of optimum COP has been explored for the parametric combination taken in the investigation.

2. DEVLOPMENT OF THE EXPERIMENTAL FACILITY

2.1. Description of the mechanical system

There are some distinct differences between the AACS and the conventional building or industrial refrigeration and air-conditioning system because of the compactness, capacity and highly variable operating conditions of the former. It has been decided to develop a stationary test facility (Figure 1) of an automotive air conditioning system by using all actual automotive components like the swash plate compressor, the microchannel heat exchangers and the thermostatic expansion valve (Table 1). Apart from these basic four components, the test rig has been equipped with some additional components like oil separator, filter/drier, sight glasses etc. They are expected to provide a better monitoring and ease of operations needed in a test rig. As in case of the original AACS, the developed test rig is also charged with R-134a.

The swash plate compressor runs at different speeds as it is driven by the engine in the car. In the test facility, instead of an engine a variable speed motor drive has been used to run the compressor via a multiple v-belt and a magnetic clutch. Polyalkylene glycol (PAG) (compatible to R-134a) is used as the lubricating oil. Though oil separators are not there in most of the automotive air conditioning systems the same has been provided in the present test bench. Separated oil is made to pass to the suction line through a capillary tube for pressure equalization.

Separate ducting arrangement has been made for condenser and evaporator to facilitate monitoring and measurement of the air stream (both flow rate and temperature). The outside walls of the ducts are insulated with

thick aeroflex sheets. Fresh air is drawn into the duct and passed through the condenser and evaporator by means of axial flow fans. In the car the fan motors receives the power supply from the automobile battery. The same arrangement is replicated in the test bench by providing a 12 volt car battery. The evaporator was kept in the original PVC casing in such a way as that the same air circuit and the flow as in the actual vehicle is replicated. To simulate the load for the air conditioning system, an electrical heater is installed downstream of the evaporator duct. Air, coming from evaporator passes over the finned electric heater which can be independently controlled by a variac. There is a provision to control the entry of fresh and recirculated air through the flap gate. Flow straighteners as well as mixers are provided at the both end of the duct. The details of the layout may be referred from Datta et al. (2013).

2.2. Selection and placement of sensors

The selection and placement of sensors are of crucial importance for the determination of steady state and dynamic characteristic of the test rig. The parameters measured in this test system include the compressor and blower speeds, refrigerant mass flow rate, the temperatures and pressures of refrigerant at different strategic points of the refrigerant loop, the air dry-bulb temperatures and relative humidity at the evaporator inlet and outlet, air temperatures at the condenser inlet and outlet, as well as air flow rate through the evaporator and through the condenser. The refrigerant mass flow rate through the system is measured by a Coriolis type mass flow meter placed in liquid line. In the present investigation, insertion types of temperature sensors have been used at a number of locations along with the surface sensors to enhance the accuracy of the measurements. The pressure drop across the condenser is also measured by a differential pressure transmitter. All the sensors give electrical outputs which are sent to a data acquisition system interfaced to a personal computer. LabVIEW (2010) platform was used for acquisition and processing of the signals. Table 2 shows the measurement devices and their accuracies used in this test system.

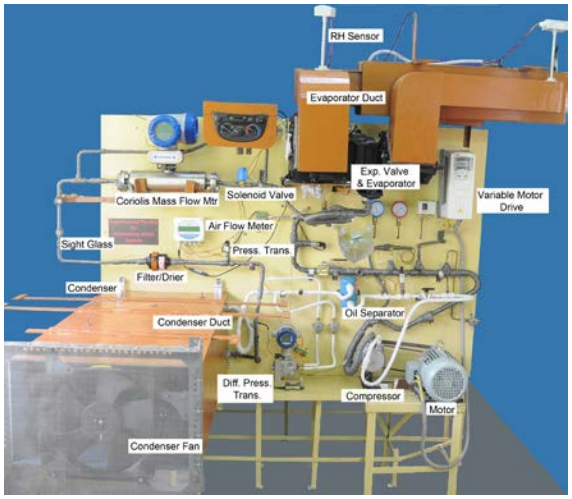

Figure 1: Photographic view of the test rig

Table 1: Details of the actual automotive HVAC components

Component	Description	Dimension/Specification
Evaporator	• Multi-flow evaporator • Fin tube type cross-flow exchanger	Size: 240mm x 197mm x 48 mm Number of tubes: 19
Condenser	• Multi-flow Condenser with fan cooling • Fin tube type cross-flow exchanger • Receiver coupled at the outlet of condenser for separating liquid refrigerants	Size: 540mm x 480mm x 163.1 mm Number of tubes: 31 Number of passes: 4; with 14, 7, 6 and 4 tubes in 1st, 2nd, 3rd and 4th pass respectively
Compressor	• Fixed displacement swash plate compressor with five pistons • Designed to be driven by engine shaft through belt drive and magnetic clutch	Type: SP08 Runs between: 800 to 2200 rpm Pressure Range: 100 to 1800 kpa
Expansion valve	Orifice type, thermostatically controlled	-
Pipe line	Pre-formed aluminium pipe	High Pressure pipe Inner Dia.: 12.35 mm Low Pressure pipe Inner Dia: 6.7 mm

2.3. Design of the Controller

In a car the Engine Control Unit (ECU) takes care of the HVAC operations along with several other important control operations. The present test rig neither contains an engine nor an ECU. A suitable controller has therefore been indigenously designed and employed with control logic as shown in Figure 2.

When the AC is switched on, the controller will first ensure that the blower is running. Then it will check the discharge pressure and the temperature recorded by the thermistor. If the discharge pressure is in between 2 to 32 Bar and the temperature is more than 4°C, the clutch of the compressor will be engaged and power will be supplied to the condenser fan; the system will start running. When the evaporator surface temperature falls to 2°C, the controller will disengage the compressor clutch to stop the system as a protection against frost formation. The next cycle of operation will commence once the evaporator surface temperature rises to 4°C again.

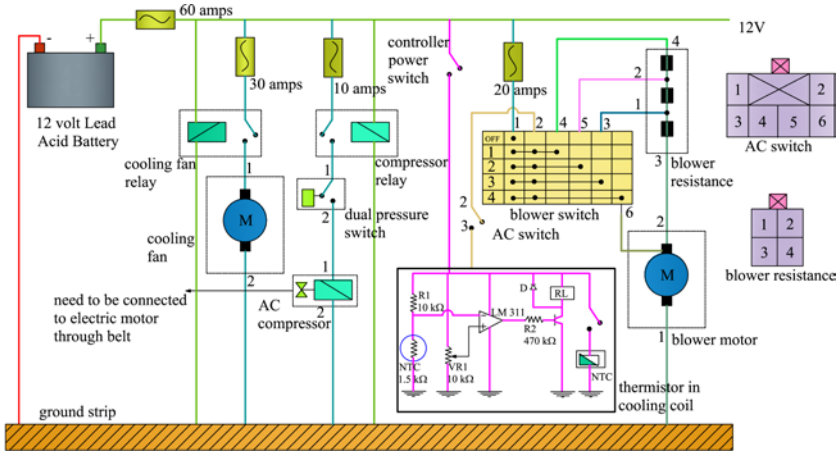

Figure 2: Controller circuit used in the test rig in lieu of ECU

Table 2: Specification of the sensors used in the test rig

Parameter	Type of sensor	Location	Accuracy
Temperature (°C)	T type thermocouple a) Surface Thermocouple b) Immersion Thermocouple c) Thermocouple matrix	a) Intermediate tube surface b) Immediately before and after main components c) Duct inlet and outlet	±0.5°C
Condenser and evaporator Pressure (Bar)	Bourdon-tube pressure gauge/ pressure transducer	Suction and discharge line	±0.25% of full scale
Condenser Pressure Drop (kPa)	Differential Pressure Transmitter	Across the condenser	±0.0375%
Refrigerant mass flow rate (kg min^{-1})	Coriolis mass flow meter	After condenser in liquid line	±2.04-0.1% of full scale (±0.75% of present reading)
Air flow rate (m s^{-1})	Hot wire based airflow transmitter	Evaporator and condenser duct	±3.0%
Relative humidity	Humidity sensor	Evaporator duct	±2.0%
Compressor speed (rpm)	Digital tachometer	Along with the motor drive	±0.025%
Thermal Image (°C)	Thermal IR imager	Condenser surface	±2.0°C

3. RANGE OF PARAMETERS, EXPERIMENTAL PROCEDURE AND UNCERTAINTY

The experiments are carried out with varying compressor and blower speed along with a variable refrigerant charge for a given ambient condition. Total sixty set of experiments are conducted at 200, 300, 400, 500 and 600 g of refrigerant charge level. In each charge level the speed of the compressor is fixed at 1000, 1300, 1600 and 1900 rpm by using the variable frequency drive. Again, for each compressor speed, the blower speed of the evaporator is

manually selected from existing control knobs at three different set points of 2208, 3092 and 3475 rpm. These respective speeds are also maintained and measured by a non-contact tachometer. In the car a battery powered fan with a fixed speed is used for condenser cooling. The performance of the condenser is directly dependent on the fan speed, which is further reliant on the charging level of the battery. Owing to this the charge of the battery is meticulously maintained to get a constant fan speed (1750 rpm, as in the car) for the entire duration of these tests. Separate measurements are made to estimate the air flow rates corresponding to each of the blower speeds. They are 64, 78 and 88 m^3h^{-1} respectively. The air flow through the condenser is 1345.5 m^3h^{-1}. Typical test runs are repeated and a good reproducibility has been observed. Utmost care has been taken to ensure more or less constant ambient air temperature and humidity during a test run and minimum possible variation in these parameters for different test runs. Experiments have been planned carefully to avoid seasonal change in ambient temperature and relative humidity. In the present test rig ambient air has been inducted through the condenser and recirculated air has been made to pass over the evaporator. The reported results are obtained during Indian summer condition with an ambient temperature and relative humidity of 34°-38°C and 55-60% at the inlet of the condenser. Whereas, the evaporator inlet air temperature and relative humidity are 28°-30°C and 30-35% respectively, which is controlled by the variation of the blower speed setting and the power supply to the electric heater. The heat load of the electric heater is kept constant at 800W by varying the power supply using a variac.

The maximum uncertainties (Moffat, 1988) of $\dot{Q}_{eva,ref}$, $\dot{W}_{comp,ref}$ and COP_{ref} at highest charge level are 1.75%, 1.76% and 4.72% respectively based on the accuracies of various measured variables presented in Table 2.

4. RESULTS

The actual thermal-hydraulic process followed by a system is immensely useful for understanding as well as assessing the system performance. On the other hand, the representation of any practical refrigeration cycle purely based on parametric measurements could be difficult as there are auxiliary components and connecting pipelines. Further, due to the physical constraints, any system will have only a limited number of measurement stations with conventional sensors (mainly for pressure and temperature). The present test rig is also not free from these limitations. Nevertheless, a simplified representation of the thermodynamic cycle followed by the system is possible based on some common assumptions such as no pressure drop across the heat exchangers and secondly, any effect of tube bends, connectors and valves has also been ignored.

4.1. Effect of refrigerant charge on suction and discharge pressure

Figure 3 depicts an increase in the suction and discharge pressure accordingly as the refrigerant charge increases whereas; it is vice versa with the increment of compressor speed. It is observed that a certain increase in the discharge pressure and a fall in the suction pressure of the system as the compressor speed increases. In case of vapor compression refrigeration cycle this is a common trend and has also been observed in earlier studies. Wang et al. (2005) reported similar trends for an automotive air conditioning system. However, as the rate of increase of discharge pressure is very moderate compared to the rate of increase of suction pressure with the increase of refrigerant charge level. From the same figures it is also obvious that the discharge pressure decreases with blower speed while the suction pressure shows a reverse trend. Increase of blower speed induces a higher load on the evaporator. The changes in suction and discharge pressure are direct outcome of that.

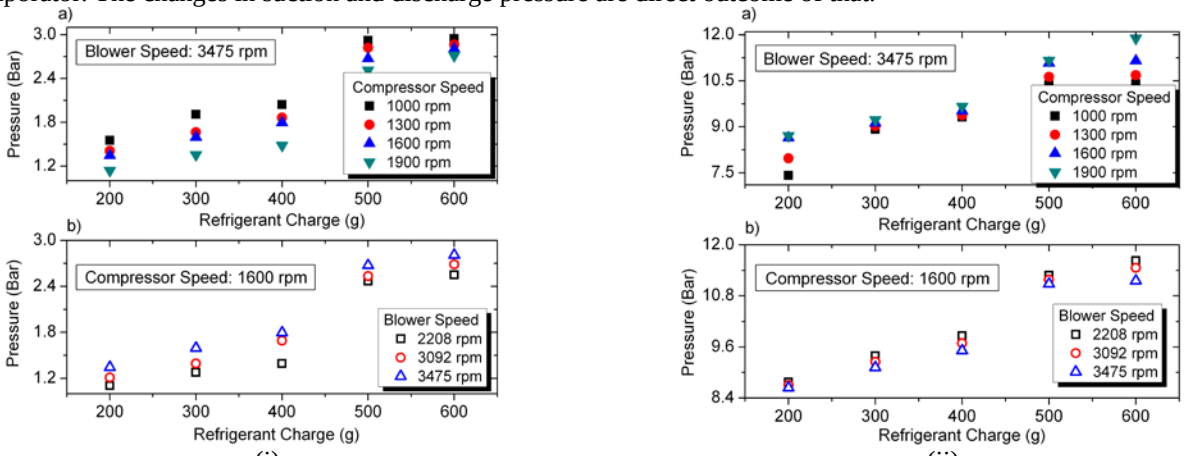

(i) (ii)

Figure 3: Effect of refrigerant charge on (i) Suction Pressure and (ii) Discharge Pressure

4.2. Effect of refrigerant charge on suction and discharge temperature

Figure 4 describes the effect of the refrigerant charge on suction and discharge temperature for different compressor speeds and blower settings. It is very obvious that both the temperature decreases with the increase of refrigerant charge. Further, suction temperature decreases with compressor speed while discharge temperature increases with it. In general, when the condenser is starving of cold airflow, the cooling of refrigerant through it will deteriorate. Alternatively, an increase in blower speed reduces discharge temperature and increases the suction temperature as shown in Figure 4. These results are also in conformity with the trend of pressure variation with compressor speed.

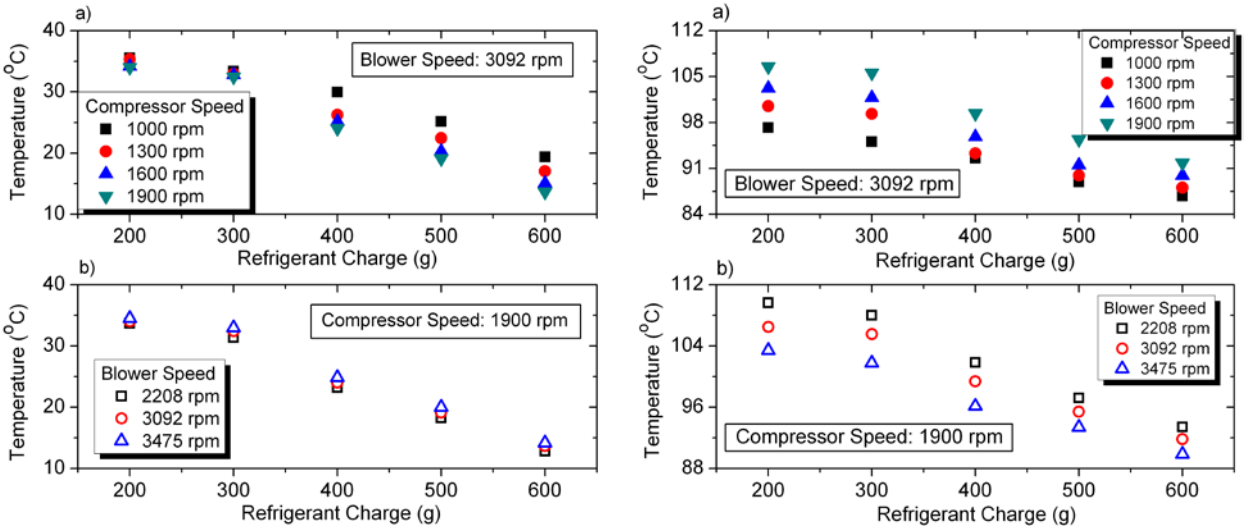

(i) (ii)

Figure 4: Effect of refrigerant charge on (i) Suction Temperature and (ii) Discharge Temperature

4.3. Effect of charge on the mass flow rate of the refrigerant

The mass flow rates through the compressor are dependent on its speed, amount of refrigerant in the system and air flow through the evaporator. The variation of mass flow rate obtained from the Coriolis mass flow meter is depicted in Figure 5 as a function of all these three. For the presented data set the maximum error in mass flow rate lies within ±0.75%. Mass flow rate increases with refrigerant charge and compressor speed as is expected. Interestingly, the variation of mass flow rate with blower speed is also noted from the experimental observations. This is for maintaining the same cooling effects through out the system.

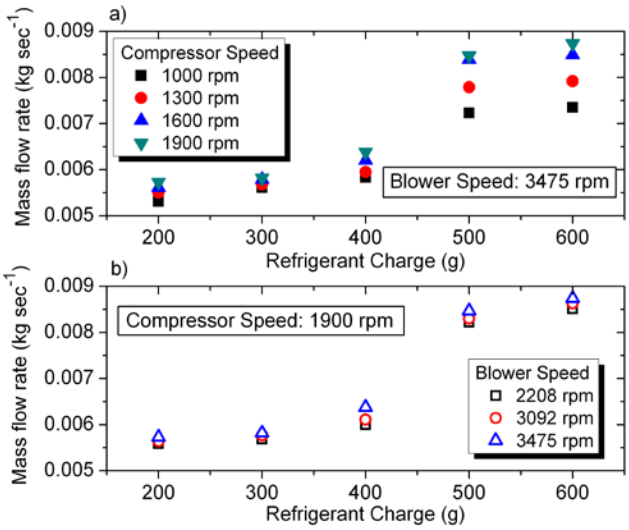

Figure 5: Effect of refrigerant charge on refrigerant mass flow rate

4.4. Effect of compressor speed on condenser surface temperature

The condenser has a typical design with a number of tube passes and varying number of tubes in each of the passes. As a result the state of refrigerant at the entry of each of the tubes is different. Further there is no guarantee that the fan forces the air uniformly over the entire face area of the condenser. These induce non-uniform cooling of the refrigerant and temperature non-uniformity of the condenser surface. Infrared images (Figure 6) of the rear face of the condenser are captured at four different compressor speeds with 500 g refrigerant charge and 3475 rpm blower speed. This is expected to provide a fairly good indication of the variation of refrigerant temperature as it flows through different tube passes. The tube passes with varying number of tubes can be easily identified along with the direction of refrigerant flow through them. Refrigerant enters to the condenser through fourteen numbers of tubes at the top left corner and leaves from the bottom left corner through four numbers of tubes. It is observed that condenser surface temperature increases with the increase of compressor speed. In each thermal image, the maximum, the minimum and the center point temperatures are highlighted.

From these thermal images, non-uniformity in condenser surface temperature is observed with the increase in compressor speed. To quantify the degree of non-uniformity, Bowers et al. (2006; 2010) introduced a rating parameter. This distribution rating parameter falls between 0 and 1; where 0 represents the highest degree of non-uniformity and 1 represents completely uniform distribution. The rating parameter ϕ can be defined in terms of the average condenser surface temperature, T_{iso}:

$$T_{iso} = \frac{\sum T_i}{M \times N} \tag{1}$$

Where, T_i is the temperature of a pixel, the total number of pixel being $M(\text{row}) \times N(\text{column})$.

Once T_{iso} is determined for a given infrared image, the image of all the N number of columns are considered. For each column, the number of pixels with temperature below T_{iso} defines a height (H_i). Again, the average height of all the columns (H_{avg}) can be found from $\sum H_i / N$. Finally, the distribution rating parameter ϕ is defined as follows:

$$\phi = 1 - \frac{\sum_{i=1}^{N} \left| H_i - H_{avg} \right|}{2NH_{avg}} \tag{2}$$

Figure 6 depicts that the distribution rating parameter along with the variation of H_i superimposed over the thermograph of the condenser surface. Distribution of H_i becomes uniform and there is a gradual increase in ϕ as the compressor speed increases. A higher mass flow rate of the refrigerant with the increase of compressor speed may be responsible for a better distribution of the fluid through the channels and an increase in the rate of heat transfer.

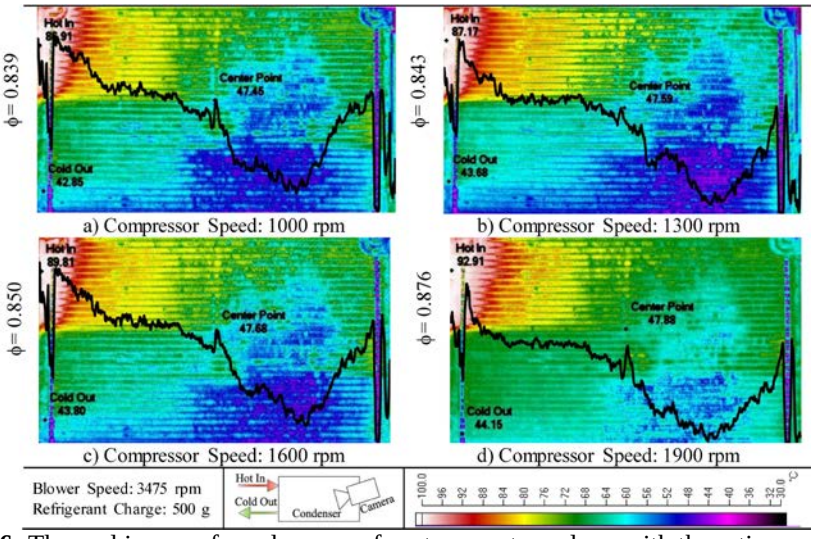

Figure 6: Thermal image of condenser surface temperature along with the rating parameter

4.5. Effect of refrigerant charge on the cooling capacity, compression work and COP

Referring to Figure 1, the cooling capacity of the evaporator can be obtained as follows:

$$\dot{Q}_{eva,ref} = \dot{m}_{comp}\left(h_{eva,out} - h_{eva,in}\right) \tag{3}$$

The cooling capacity increases both with the increase in compressor and blower speeds, though the effect of blower speed is not as pronounced as it is in the case of compressor speed (Figure 7a). The increase in mass flow rate with compressor speed also enhances the cooling capacity. Similarly, the increased air flow rate at higher blower speed increases the cooling capacity. It is intuitive that the cooling capacity of an air conditioning system will increase with the increase of refrigerant charge up to certain level. Further increment of refrigerant charging deteriorates the cooling capacity of the system. As seen from Figure 7a, an optimal value of cooling capacity is obtained near a refrigerant mass charge of 530±3 g. It is observed that the optimal condition corresponds approximately to a state having the condenser outlet at a certain amount of subcooling. In addition, the refrigerant overcharge may overheat the suction temperature and decrease the effective cooling capacity which will cause a pronounced performance drop.

One may also estimate the cooling capacity from the air side heat transfer. For a well-insulated experimental facility both the estimation should match within the range of experimental errors. On the other hand, work done by the compressor can be estimated as follows,

$$\dot{W}_{comp} = \dot{m}_{comp}\left(h_{comp,out} - h_{comp,in}\right) \tag{4}$$

Compression work increases both with the compressor speed and refrigerant charge (Figure 7b). As with the increase of speed and charge level, mass flow rate and the pressure ratio of the compressor increases, its direct consequences can be felt as the increase in compressor speed. So, the combined effect of these two parameters gives a substantial rise in compression work. It is interesting to note that, though there is an increase in refrigerant mass flow through the circuit, the enthalpy difference between the inlet and outlet of the compressor decreases drastically with the blower speed to ultimately reduce the compression work.

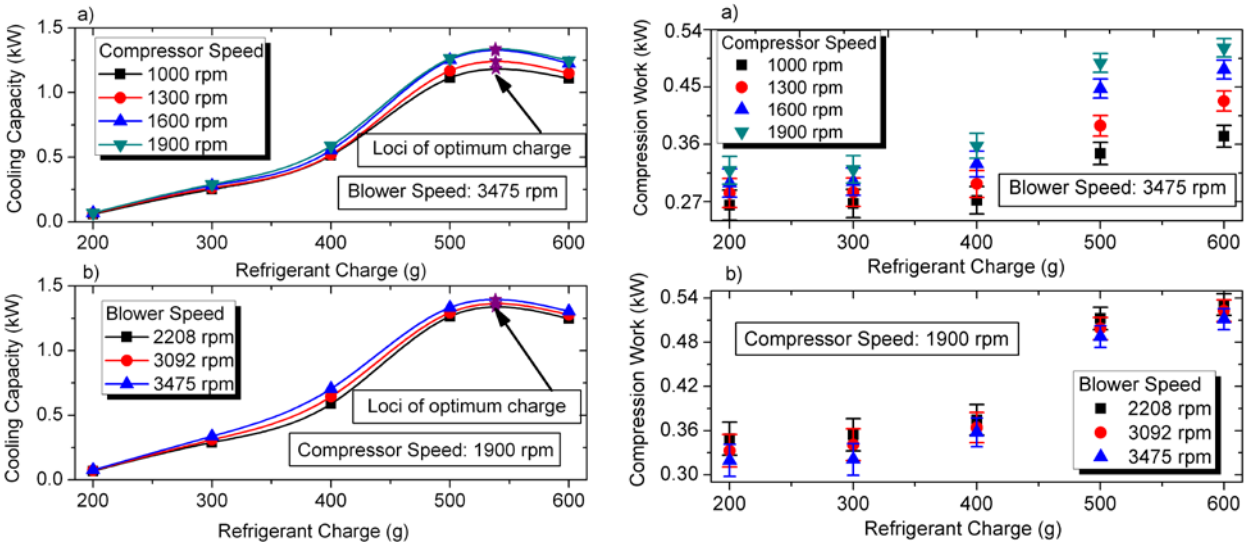

(a) (b)

Figure 7: Effect of refrigerant charge on system (a) Cooling Capacity and (b) Compression Work

Finally, the COP of the system over a wide range of experimental parameters has been depicted in Figure 8. As COP is the ratio of cooling capacity to compression work, increase of refrigerant charge and blower speed is expected to increase COP considerably as the pattern of cooling capacity. It is observed from Figure 7(a) and 7(b) that the rates of increase of compression work is much more compared to the rate of cooling capacity at any speed of the compressor. It depicted on the performance of COP of the system by decreasing with the compressor speed. Initially, the COP increases with the refrigerant charge, but after the optimal charge level it decreases. The sharp rise is associated with the effective cooling capacity caused by the effective latent heat transport in the two phase region

of refrigerant flow. Further increase of refrigerant charge creates a certain flooding in the condenser that may result in higher system pressure.

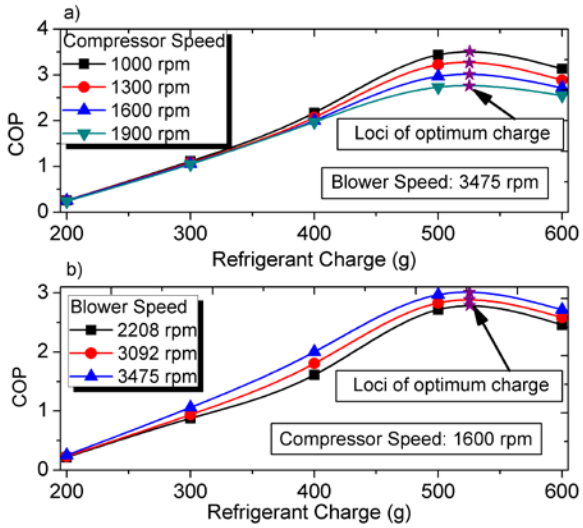

Figure 8: Effect of refrigerant charge on system COP

5. CONCLUSIONS

A stationary test bench has been developed for the investigation of steady state and dynamic performance of an automotive air conditioning system. The test facility replicates the hardware arrangement of the actual automobile as far as practicable and uses the components used in the actual system. As the engine is absent in the facility the variation of the compressor speed is achieved through a variable frequency motor which engages with the compressor through a magnetic clutch. Additionally, an indigenously designed controller has been used in the test facility. It actuates the magnetic clutch following the protocols for safety and drive sequence of the fan (condenser) and blower (evaporator) motors exactly as it is done in the car. The facility also contains a large number of sensors in excess to those few present in the actual system. The steady state performance of the system has been investigated for three independent variables, namely the refrigerant charge level, the compressor speed and the speed of the evaporator fan as they are the only variable parameters for a running car. The following trends have been observed.

- The suction and discharge pressure increases with the increase of refrigerant charge whereas, the suction and discharge temperature decreases with the charge amount.
- The discharge pressure and temperature increases with the increase of compressor speed.
- Suction pressure and temperature increases with the increase of blower speed accompanied by a decrease in discharge pressure and temperature.
- A distribution rating parameter has been calculated to quantify the temperature non-uniformity in the condenser as well as the effective use of the available heat transfer area through the use of infrared thermography.
- With the increase of compressor speed, cooling load and compression work increases whereas, COP of system decreases.
- With the increase of refrigerant charge cooling capacity and COP of the system increases up to a certain range then, it decreases whereas, the compression work continuously increases with the refrigerant charge.
- Irrespective of the compressor and the blower speed, the optimum performance of cooling capacity and COP of the system lies in between the refrigerant charge of 530±3 g.

The optimal performance of the system is not only dependent on the system COP; rather it is also dependent on its suction temperature. The refrigerant overcharge decreases the suction pressure and temperature which will significantly increase the degree of superheat and eventually decrease the cooling capacity by more than 15%.

NOMENCLATURE

AACS	Automotive Air Conditioning System	(-)	**Subscripts**	
COP	Coefficient of Performance	(-)	avg	Average
h	Enthalpy	(kJ kg^{-1})	comp	Compressor

$\dot{m}$	Mass flow rate	(kg sec^{-1})	eva	Evaporator
N	Number of columns	(-)	in	Inlet
$\dot{Q}$	Cooling capacity	(kW)	iso	Isotherm
T	Temperature	(^{o}C)	out	Outlet
$\dot{W}$	Compressor work	(kW)	ref	Refrigerant
H	Height	(Pixels)		
ϕ	Distribution rating parameter	(-)		

REFERENCES

Atik, K., Aktas, A., Deniz, E., 2010, Performance parameters estimation of MAC by using artificial neural network, *Expert Syst. Appl.* Vol. 37, no. 7: p. 5436–5442.

Bhatti, M.S., 1999, Riding in comfort, Part II: Evolution of automotive air conditioning, *ASHRAE J.*, vol. 41, no. 9: p. 44–52.

Bowers, C.D., Hrnjak, P.S., Newell, T.A., 2006, Two-Phase Refrigerant Distribution in a Microchannel Manifold, *International Refrigeration and Air Conditioning Conference at Purdue*, Paper # R161.

Bowers, C.D., Wujek, S.S., Hrnjak, P.S., 2010, Quantification of refrigerant distribution and effectiveness in microchannel heat exchangers using infrared thermography, *International Refrigeration and Air Conditioning Conference at Purdue*, Paper # 2117.

Datta, S.P., Das, P.K., Mukhopadhyay, S., 2013, Performance of an off-board test rig for an automotive air conditioning system, *Int. J. of Air-Cond. and Refrig.*, vol. 21: p. 1350020.

Forrest, W.O., Bhatti M.S., 2002, Energy efficient automotive air conditioning system, *SAE 2002 World Congress*, Detroit, Michigan.

Gu, J., Kawaji, M., Smith-Pollard, T., Cotton, J., 2003, Multi-channel R134a two-phase flow measurement technique for automobile airconditioning system, *4th ASME/FED & JSME Fluids Engineering Division Summer Meeting*, Honolulu, Hawii, USA.

Hosoz, M., Direk, M., 2006, Performance evaluation of an integrated automotive air conditioning and heat pump system, *Energ. Convers. Manag.*, vol. 47, no. 5: p. 545–559.

Hosoz, M., Ertunc, H.M., 2006, Artificial neural network analysis of an automobile air conditioning system, *Energ. Convers. Manag.*, vol. 47, no. 11-12: p. 1574–1587.

Jabardo, J.M.S., Mamani, W.G., Ianella, M.R., 2002, Modelling and experimental evaluation of an automotive air conditioning system with a variable capacity compressor, *Int. J. Refrig.*, vol. 25, no. 8: p. 1157–1172.

Kamar, H.M., Ahmadb, R., Kamsah, N.B., Mustafa, A.F.M., 2013, Artificial neural networks for automotive air-conditioning systems performance prediction, *Appl. Therm. Eng.*, vol. 50, no. 1: p. 63-70.

Kargilis, A., 2003, Design and development of automotive air conditioning systems, *ALKAR Engineering Company*.

Kaynakli, O., Horuz, I., 2003, An experimental analysis of automotive air conditioning system, *Int. Comm. in Heat and Mass Transfer*, vol. 30, no. 2: p. 273–284.

Khayyam, H., 2013, Adaptive intelligent control of vehicle air conditioning system, *Appl. Therm. Eng.* vol. 51, no. 1-2: p. 1154-1161.

Khayyam, H., Abawajy, J., Jazar, R.N., 2012, Intelligent energy management control of vehicle air conditioning system coupled with engine, *Appl. Therm. Eng.*, vol. 48, p. 211-224.

Khayyama, H., Kouzani, A.Z., Hu, E.J., Nahavandi, S., 2011, Coordinated energy management of vehicle air conditioning system, *Appl. Therm. Eng.*, vol. 31, no. 5: p. 750-764.

Lee, G.H., Loo, J.Y., 2000, Performance analysis and simulation of automobile air conditioning system, *Int. J. Refrig.*, vol. 23, no. 3: p. 243–254.

Moffat, R.J., 1988, Describing the uncertainties in experimental results, *Exp. Therm. Fluid Sci.*, vol. 1, no. 1: p. 3–17.

National Instruments, LabVIEW-2010 (2010), http://www.ni.com/labview/ .

Park, Y.C., McEnaney, R., Boewe, D., Yin, J.M., Hrnjak, P.S., 1999, Steady state and cycling performance of a typical R134a mobile A/C system, *SAE Congress Proceeding*, SAE Tech. Paper 1999-01-1190.

Qi, Z., Chen, J., Chen, Z., Hu, W., He, B., 2007, Experimental study of an auto-controlled automobile air conditioning system with an externally-controlled variable displacement compressor, *Appl. Therm. Eng.*, vol. 27, no. 5-6: p. 927–933.

Ratts, E.B., Brown, J.S., 2000, An experimental analysis of cycling in an automotive air conditioning system, *Appl. Therm. Eng.*, vol. 20, no. 11: p. 1039–1058.

Trzebinski, D., Szczygiel, I., 2010, Thermal analysis of car air conditioning, *Archives of Thermo.*, vol. 31, no.4: p. 71-80.

Wang, S., Gu, J., 2004, Experimental analysis of an automotive air conditioning system with two-phase flow measurements, *10th Int. Refrigeration and Air Conditioning Conference at Purdue*.

Wang, S., Gu, J., Dickson, T., Dexter, J., McGregor, I., 2005, Vapor Quality and Performance of an Automotive Air Conditioning System, *Exp. Therm. Fluid Sci.*, vol. 30, no. 1: p. 59–66.

ACKNOWLEDGEMENT

The authors gratefully acknowledge the financial support of General Motors India Science Lab Bangalore under the aegis of the General Motors-IIT Kharagpur Collaborative Research Laboratory.